Hindawi Publishing Corporation
Mathematical Problems in Engineering
Volume 2014, Article ID 920480, 8 pages
http://dx.doi.org/10.1155/2014/920480

Research Article

Numerical Investigation of Water Droplets Shape Influence on Mathematical Modeling Results of Its Evaporation in Motion through a High-Temperature Gas

Dmitrii O. Glushkov, Genii V. Kuznetsov, and Pavel A. Strizhak

National Research Tomsk Polytechnic University, 30 Lenin Avenue, Tomsk 634050, Russia

Correspondence should be addressed to Dmitrii O. Glushkov; dmitriyog@tpu.ru

Received 6 November 2013; Accepted 28 April 2014; Published 18 May 2014

Academic Editor: Shaoyong Lai

The numerical investigation of influence of a single water droplet shape on the mathematical modeling results of its evaporation in motion through high-temperature gases (combustion products of a typical condensed substance) has been executed. Values of evaporation time, motion velocity, and distance passed by various droplet shapes (cylinder, sphere, hemisphere, cone, and ellipsoid) in a high-temperature gases medium were analyzed. Conditions have been defined when a droplet surface configuration affects the integrated characteristics of its evaporation, besides temperature and combustion products concentration in a droplet trace, insignificantly. Experimental investigations for the verification of theoretical results have been carried out with using of optical diagnostic methods for two-phase gas-vapor-liquid flows.

1. Introduction

Opportunity of significant efficiency of the flame localization and the firefighting with using water spray is substantiated by numerous studies, for example, [1–5]. Attention is traditionally focused on experimental study [3–5] of physicochemical processes, which often differs from the actual fire situations, under the laboratory conditions. Also there had been a try at theoretical regularities study [1, 2] of the firefighting with water spray. It has been marked that [1, 2] the numerical investigations with using corresponding models of heat and mass transfer and phase transformations are expedient.

In recent years, the group of heat and mass transfer models [6–8] in water droplet motion through high temperature gases has been developed. Its gases were some combustion products mixed with water vapor. However, the results are not ample for developing science-based technologies of the effective firefighting with using water spray [6–8]. The term "effective firefighting" means that the evaporation is completed and the fire is eliminated.

There are a lot of problems requiring solutions. One of them is an appraisement of a water droplet shape influence in its motion through high-temperature gases medium on evaporation characteristics. It is common knowledge [9, 10] that moving water droplets are deforming permanently. Accordingly, as a result of changing the water droplet shape, the coefficient of resistance c_χ is changing. Its numerical value depends on moving body configuration.

Description of an accurate droplet shape border under the conditions of its evaporation in the high-temperature gases medium, when heat and mass transfer problems should be determined numerically, is a separate problem. But difficulties of methodological support of procedure considering the droplet shape are not the main. Such problems for hemisphere, semicylinder, and cylinder have solutions [11, 12]. The main problem is the big time expenditure for its numerical solutions, which can be compared with other numerical solutions all in all (relating with solving the unsteady differential equations system [11, 12]).

So the numerical analysis of correlation between the water droplet shape and integrated characteristics of its evaporation (evaporation time, motion velocity, overcome distance, gas temperature, and water vapor concentration in droplet trace, and others) in motion through high-temperature gases medium is expedient.

The aim of this work is a numerical investigation for influence of typical water droplet shapes (cylinder, sphere, hemisphere, cone, and ellipsoid) on characteristics of its evaporation in motion through high-temperature combustion products.

2. Problem Statement and Mathematical Model

Figure 1 shows the scheme of solution domain of heat and mass transfer problem for single water droplet in motion through high-temperature gases. Combustion products of typical oil fuel, kerosene, have been considered similarly [6–8].

In modeling we accepted that the initial water droplet temperature T_0 was significantly lower than the gases temperature T_f that was equal to the average temperature 1170 K of the fire. It was considered that the droplet was warming due to heat conduction. There was the evaporation on the border "liquid-gas" ($z = Z_1$, $z = Z_2$, $0 < r < R_1$; $r = R_1$, $Z_1 < z < Z_2$). Water vapors were injected into the high-temperature gases medium and mixed with gases. Vapor-gas mixture temperature near droplet motion trajectory lowered because of endothermic phase transition heat and vapor injection. Droplet dimension decreased under the conditions of the intensive evaporation. In due course evaporation was completed. The droplet existence time from the beginning of droplet motion through gases medium to the end of its evaporation was τ_d.

In realization of numerical studies [6–8] the correlation between the droplet existence time and its initial dimensions has been established. In the system (Figure 1) droplet dimensions were selected if average time of droplet complete evaporation has been achieved. Droplet dimensions were selected from [6–8] and they were $R_d = 0.25 \cdot 10^{-3}$ m, $Z_d = 10^{-3}$ m.

In formulating heat and mass transfer problem (Figure 1) we assumed the following assumptions.

(1) Gases medium is binary. It is the "combustion products- (smoke-gases-) water vapor" system. In numerical modeling a smoke-gases component structure is not detailed, because its changes for combustion process of wide group of substances and materials are not considerable. Detailed analysis of the smoke-gases component structure is the independent difficult scientific problem. So in numerical modeling of heat and mass transfer process and phase transition in the system (Figure 1) the use of binary mixture with known components model is expedient.

(2) In numerical solution of heat and mass transfer problem it is considered the cylindrical droplet shape (Figure 1). It is established [6–8] that cylinder (Figure 2) is the closest actual interpretation of droplet configuration of possible variants. The symmetry axis of the cylinder coincides with vector direction of the droplet motion. At any time it is possible to select such cylinder dimension when its surface medium equals droplet surface medium (Figure 2).

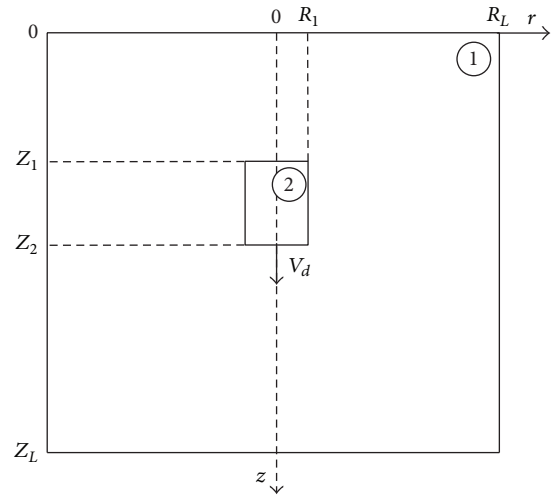

Figure 1: A scheme of the solution domain. 1: high-temperature gas; 2: water droplet.

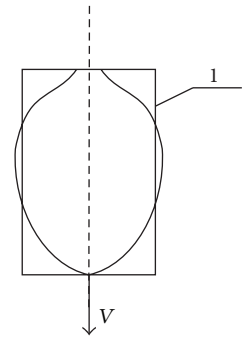

Figure 2: A scheme of a moving droplet. 1: droplet of a cylinder shape.

Preliminary analysis of droplet evaporation conditions shows that the shape of droplet with constant surface medium does not influence intensity of the evaporation process and accordingly temperature fields and water vapor concentration in its trace and in the vicinity of the phase transition border. But the droplet shape influences its motion velocity. The coefficient of the motion resistance c_χ changes because of changing droplet shape. So in numerical modeling of process under study it is expedient to consider some variants of coefficient numerical values c_χ under identical initial information. Thus, it is possible to analyze the influence of droplet aerodynamic characteristics on the water vapor curtain formation in its trace.

(3) Deformation of droplet surface is not considered. Video frames analysis [10, 11] allows us to conclude that it is impossible to consider the droplet shape dynamic change, which was a result of its surface deformation in numerical modeling. Also the investigations [10, 11] show that

during the droplet surface deformation the total evaporation medium does not remain constant practically (only the reduction of droplet dimensions in due course takes place as a result of evaporation).

(4) Possible droplet destruction is not considered. When the droplet velocity (significantly subsonic) and dimensions are low and the complete evaporation time is short ($\tau_d < 1$), decay probability is extremely low. It was established [6–8] that for the conditions in question the Weber number by varying the basic parameters in wide ranges does not exceed 1. If We < 1 the droplet destruction terms (decay) or the water droplet crushing is not realized.

(5) Thermophysical characteristics of the substances (water droplet, combustion products, water vapor) are not depending on the temperature. So analysis of results [6–8] enables us to infer that with the first approximation this factor can be neglected for the temperature range under consideration.

The mathematic model, corresponding to the adopted problem statement (Figure 1), includes the next nonstationary system of nonstationary differential equations with partial derivatives ($0 < \tau < \tau_d$). Consider the following.

Heat transfer equations for vapor-gases mixture and water droplet:

$$\begin{gathered} 0 < r < R_L, \quad 0 < z < Z_1, \quad Z_2 < z < Z_L; \\ R_1 < r < R_L, \quad Z_1 < z < Z_2 \\ C_1\rho_1 \frac{\partial T_1}{\partial \tau} = \lambda_1 \left[\frac{\partial T_1^2}{\partial r^2} + \frac{1}{r}\frac{\partial T_1}{\partial r} + \frac{\partial T_1^2}{\partial z^2} \right], \\ 0 < r < R_1, \quad Z_1 < z < Z_2 \\ C_2\rho_2 \frac{\partial T_2}{\partial \tau} = \lambda_2 \left[\frac{\partial T_2^2}{\partial r^2} + \frac{1}{r}\frac{\partial T_2}{\partial r} + \frac{\partial T_2^2}{\partial z^2} \right], \end{gathered} \tag{1}$$

diffusion and vapor-gases mixture balance equations:

$$\begin{gathered} 0 < r < R_L, \quad 0 < z < Z_1, \quad Z_2 < z < Z_L; \\ R_1 < r < R_L, \quad Z_1 < z < Z_2 \\ \frac{\partial \gamma_w}{\partial \tau} = D_3 \left[\frac{\partial \gamma_w^2}{\partial r^2} + \frac{1}{r}\frac{\partial \gamma_w}{\partial r} + \frac{\partial \gamma_w^2}{\partial z^2} \right], \\ \gamma_f + \gamma_w = 1. \end{gathered} \tag{2}$$

Here τ is time, s; τ_d is time of full droplet evaporation, s; r and z are coordinates of the cylindrical system, m; R_L and Z_L are solution domain dimensions, m; C is a specific heat, J/(kg·K); ρ is a density, kg/m^3; T is a temperature, K; λ is a thermal conductivity, W/(m·K); γ_w is the dimensionless concentration of water vapors; D is the diffusion coefficient, m^2/s; γ_f is the dimensionless concentration of gases (combustion products); subscripts 1, 2, and 3 correspond to a vapor-gases mixture, a water droplet, and a water vapor.

The initial conditions ($\tau = 0$) are $T = T_0$ at $0 < r < R_1$, $Z_1 < z < Z_2$; $T = T_f$, $\gamma_f = 1$, $\gamma_w = 0$ at $0 < r < R_L$, $0 < z < Z_1$, $Z_2 < z < Z_L$; $R_1 < r < R_L$, $Z_1 < z < Z_2$.

The boundary conditions were similar [6–8]. On boundaries "liquid-gas" ($r = R_1$, $Z_1 < z < Z_2$; $z = Z_1$, $z = Z_2$, $0 < r < R_1$) evaporation was taken into account. On the symmetry axis ($r = 0$, $0 < z < Z_L$) and external boundaries ($r = R_L$, $0 < z < Z_L$; $z = 0$, $z = Z_L$, $0 < r < R_L$) for all of the equations, we set the condition of gradients vanishing of the corresponding functions.

On all droplet sides influence of water vapors blowing on heat exchange conditions was considered. Therefore the following boundary conditions were exposed for the heat transfer equations [6–8]:

$$\begin{gathered} T_1 = T_2, \\ \lambda_2 \frac{\partial T_2}{\partial r} = \lambda_1 \frac{\partial T_1}{\partial r} - Q_e W_e - \rho_3 C_3 V_e \left(T_{3s} - T_{2s}\right) \\ \text{at } r = R_1, \ Z_1 < z < Z_2, \\ T_1 = T_2, \\ \lambda_2 \frac{\partial T_2}{\partial z} = \lambda_1 \frac{\partial T_1}{\partial z} - Q_e W_e - \rho_3 C_3 V_e \left(T_{3s} - T_{2s}\right) \\ \text{at } z = Z_1, \ z = Z_2, \ 0 < r < R_1, \end{gathered} \tag{3}$$

where Q_e is the thermal reaction coefficient of evaporation, J/kg; W_e is the mass velocity of evaporation, kg/(m^2·s); V_e is the velocity of water vapors from the corresponding droplet surface, m/s; T_{2s} and T_{3s} are the temperature of water and vapors in the vicinity of the phase transition border, K.

The equation of a droplet motion (Figure 1) with allowance for action of resistance force and gravity, evaporation on a surface of a body in flow, convective currents in a droplet, and also its relative acceleration has the following appearance in accordance with [13–19]:

$$\begin{aligned} \frac{dV_d}{d\tau} = {} & \frac{3\rho_3}{4\rho_2 2R_d} c_\chi \frac{1}{B+1} \frac{1 + (2/3)\left(\mu_2/\mu_3\right)}{1 + \mu_2/\mu_3} \\ & \times (A+1)^{1.2\pm0.03} \left|V_d - V_e\right| \left(V_d - V_e\right) + g, \end{aligned} \tag{4}$$

where V_d is the droplet motion velocity, m/s; c_χ is a dimensionless resistance coefficient [14–17]; B is the Spalding transfer number [18]; μ is the coefficient of dynamical viscosity, kg/(m·s); A is the dimensionless complex characterizing relative droplets acceleration [19]; R_d is the droplet radius, m; g is the gravitational acceleration, m/s^2.

To compute the mass velocity of water droplet evaporation, we used the following expression [20]:

$$W_e = \frac{\beta}{1 - k_\beta \beta} \frac{\left(P^n - P\right)}{\sqrt{2\pi R_t T_{2s}/M}}, \tag{5}$$

where β is the dimensionless coefficient of condensation (evaporation); k_β is the dimensionless coefficient ($k_\beta \approx 0.4$ [20]); P^n is the pressure of saturated water vapor, N/m^2; P is the pressure of water vapor near the phase transition border, N/m^2; M is the painting mass of water, kg/kmol.

The set of the nonstationary differential equations (1)-(2) is solved by the method of finite differences [21]. Algorithms

[6–8] were used. The reliability of the obtained results was verified by the test of conservatism of the utilized difference schemes, whose algorithm is given by [6–8].

3. Results and Discussion

Numerical investigations of heat and mass transfer processes and phase transformations in the system in question (Figure 1) have been carried out for the following typical values: initial water droplet temperature $T_0 = 300$ K; gases temperature $T_f = 1170$ K; thermal effect of water evaporation $Q_e = 2.26 \cdot 10^6$ J/kg; droplet dimensions $R_d = 0.25 \cdot 10^{-3}$ m, $Z_d = 10^{-3}$ m; solution domain dimensions $R_L = 0.1$ m, $Z_L = 1$–4 m; initial droplet motion velocity $V_0 = 0.5$ m/s; molar mass of water $M = 18$ kg/kmol; dimensionless ratio of condensation (evaporation) $\beta = 0.1$. Thermophysical characteristics of water, gases (combustion products), and water vapor were adequate [6–8].

The influence analysis of water droplet surface configuration on its integral evaporation characteristics has been performed by the variation coefficient of resistance c_χ in a wide range, corresponding to the most typical shapes of free moving water droplets [14–17]. Under the selected parameters of heat and mass transfer processes c_χ were [14–17]: semisphere—$c_\chi = 0.42$, sphere—$c_\chi = 0.47$, cone—$c_\chi = 0.5$, ellipsoid—$c_\chi = 0.54$, and cylinder—$c_\chi = 0.82$. Also terms when $c_\chi \to 1$ (numerical modeling is performed under $c_\chi = 0.98$ corresponding cube shape bodies) have been considered. Selected shapes most of all are used in numerical motion modeling of different particles and droplets in the liquid and gases flows, for example, [22–25].

It has been established that time of complete droplet evaporation changed unsubstantially if c_χ increased from 0.42 up to 0.98 (Table 1). Departures from τ_d were not exceeding 2%. Values V_d and L_d are changed more than τ_d (Table 1). For example, departures V_d were 9.5% and departures L_d were 6.5%. The obtained results are attributable to that fact that, under c_χ increasing, resistance force increases and V_d reduces. As a consequence L_d decreases (Table 1).

It is important that in spite of some changes of V_d and L_d the complete evaporation time τ_d, which were received by variation of c_χ, changes unsubstantially (Table 1). It is conditioned by the dominant phase transition influence on the droplet lifetime [6–8]. Under the conditions of the great gases temperatures ($T_f = 1170$ K), the mass evaporation velocity stays very high and linear velocity of the water vapor blowing in boundary layer of moving droplet V_e is comparable with V_d as a numerical value, respectively. This takes place in spite of some changes of blowing surface configuration. Under the conditions of the intensive evaporation and blowing the contribution of the first summand of (4) becomes small than its second summand (g = const). The change of c_χ influences acceleration $dV_d/d\tau$ insignificantly, respectively. This is shown in Table 1. As a consequence in evaporation the droplet dimension reduction occurs in a time τ_d, close to some of the most typical shapes of bodies in flow.

Figures 3 and 4 show isotherms and isolines of water vapor concentration for c_χ, corresponding bottom ($c_\chi = 0.42$) and top ($c_\chi = 0.98$) limit of the range resistance coefficient variation.

Table 1: Characteristics of a water droplet evaporation at different values of coefficient c_χ.

c_χ	0.42	0.47	0.50	0.54	0.82	0.98
τ_d, s	0.468	0.469	0.469	0.470	0.475	0.477
V_d, m/s	4.911	4.879	4.852	4.822	4.593	4.453
L_d, m	2.241	2.233	2.229	2.221	2.149	2.106

According to obtained isotherms (Figure 3) it is obvious that under the increase of the resistance coefficient c_χ the droplet trace width increases slightly (up to 10%). However under c_χ changes from 0.42 up to 0.98 (the influence of heat absorption during the phase transfer on gases temperature in trace decreases) gases temperature values in droplet trace (on the symmetry axis $r = 0$) increase by 6%. Similar regularity (Figure 4) can be singled out for concentration isolines γ_w. Trace width decreases (up to 12%) and absolute values γ_w (on the symmetry axis $r = 0$) increase by 7% for lowering c_χ. The obtained results are attributable to the fact that under the increase of c_χ, resistance force influence on droplet motion terms increases. Droplet motion velocity through the high-temperature gases medium is lowered. Gases cooling zone transversely relative to the motion trajectory increases. These taken place because the influence of endothermic phase transition on heat sink terms increases and combustion products absorb more energy. As a consequence the typical dimensions of "temperature" (Figure 3) and "concentration" (Figure 4) water droplet traces increase (up to 12%) slightly.

Nonetheless it is important that values of gases temperature (Figure 3) and water vapor concentration (Figure 4), obtained by significant variation of resistance coefficient (deviations γ_w and T in solution domain are not exceeded 10%), are very close. It also is attributable to the fact that if evaporation mediums equal each other under the conditions of the high temperatures, masses of water vapor, blowing from different shapes of droplet surface, they are very close. Evaporation velocity, linear velocity of the water vapor blowing in boundary layer of droplet, temperature close by phase transition border (Figure 3), and concentration γ_w (Figure 4) in droplet trace are compared. As a consequence the integral characteristics (lifetime, motion distance, and motion velocity) of droplet evaporation (not more than 9.5%), gases temperature (up to 6%), and water vapor concentration in its trace (up to 7%) differed insignificantly (Table 1).

For verification of theoretical results the experimental investigations of integrated characteristics of water droplet evaporation in the high-temperature gases medium with using of optical methods diagnostic of two-phase gas-vapor-liquid flows have been carried out, "particle image velocimetry" (PIV) and "interferometric particle imaging" (IPI) [26–28]. Figure 5 shows the scheme of experimental plant.

Combustion products of typical oil fuel, kerosene (filled the cylindrical channel 13), were considered as high-temperature gases (the same as model representation). Gases temperature in cylinder 13 was controlled by three chromel-alumel thermocouples 17, which had been installed on

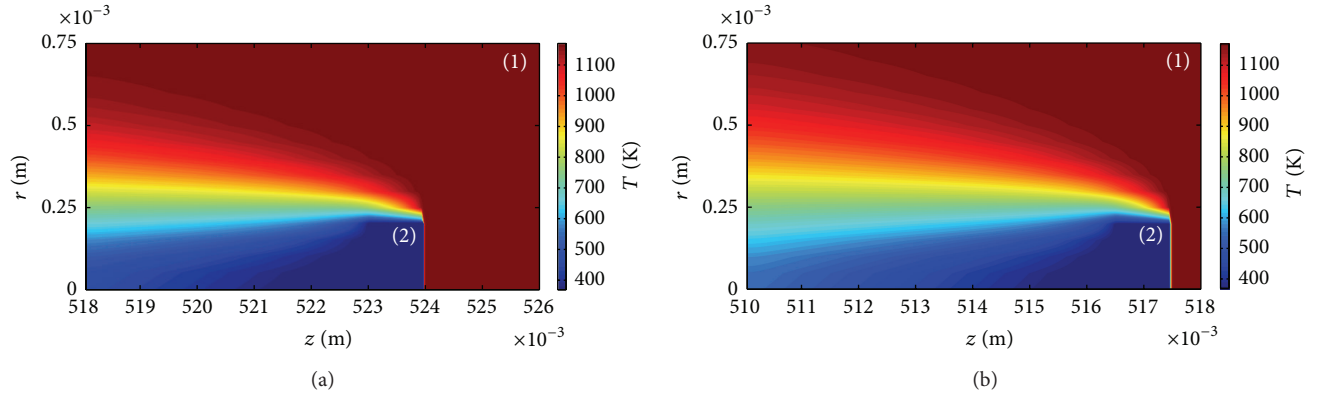

FIGURE 3: Isotherms (T, K) at $c_\chi = 0.42$ (a) and $c_\chi = 0.98$ (b) ($\tau = 0.15$ s, $R_d = 0.25 \cdot 10^{-3}$ m, $Z_d = 10^{-3}$ m). 1: high-temperature gases; 2: droplet.

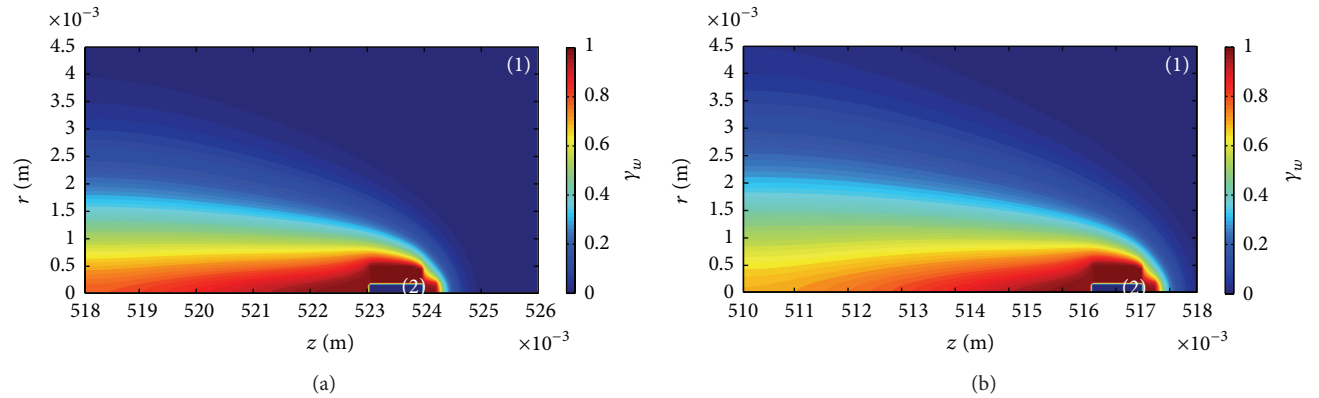

FIGURE 4: Isolines of water vapor concentration (γ_w) in a trace of moving droplet at $c_\chi = 0.42$ (a) and $c_\chi = 0.98$ (b) ($\tau = 0.15$ s, $R_d = 0.25 \cdot 10^{-3}$ m, $Z_d = 10^{-3}$ m). 1: high-temperature gases; 2: droplet.

different heights of channel (0.15 m; 0.5 m; 0.85 m). Thermocouple sensing elements in the channel were placed in that way those measurements were conducted on channel symmetry axis. Moreover, temperature gradients over the cross section were analyzed before experiments (thermocouple sensing elements were moved to channel side relatively of symmetry axis). It has been established that maximum gases temperature deviations everywhere were about 30 K relative to some average value 1080 K.

Initial water temperature was measured before it was supplied in vessel 7 of the experimental plant. It was 293 ± 2.5 K (chromel-copel thermocouple used).

Laser trajectory radioscopy procedure of water droplets motion was performed for fixation images of this motion. Preliminary experiments showed that it was necessary to use special additives (admixtures) conducive to increase of contrast images of water droplets moving in high-temperature gases medium. So "tracers" (particles of titanium dioxide powder with granule dimensions not more than 10^{-8} m) were added into the water. Minimal (up to 5%) concentration TiO_2in water was provided. It was enough to obtain a clear "spot light" in camera focus. In experiments the titanium dioxide was used, since it did not dissolve in water and has little effect under the conditions of water evaporation.

Dosing device 9, which is rendered possible to regulate the velocity of droplet injection and the characteristic dimension, conditional droplet radius in ellipsoid shape ($0.5 \cdot 10^{-3} < R_d < 5 \cdot 10^{-3}$ m), was used for droplet formation. The metrology system was used for image registration of moving droplets. This system consists of laser generator 3, solid state lasers for ultrashort pulses 4, cross-correlation digital camera 5, synchronizer 2, andpersonal computer 1 with application software rendering possible framing results (timeout between shots for tracking droplet motion within registry domain was equal to $0.1 \cdot 10^{-3}$ s).

Experiments were performed in two stages. On the first stage, the main primal problem was the registration of droplet dimension and velocity, generated by dosing device. The tuning of flat and typical characteristic dimensions (conditional radius) of emitted droplets R_d (up to $5 \cdot 10^{-3}$ m) was performed for the group of practical application. Laser-illuminated droplet images were fixed by cross-correlation digital camera. Its focus was directed perpendicular to "light pulse."

Water droplet dimension in the computational domain was determined by the optical method IPI [27]. In registry domain water droplets were lighted by the "light pulse" 6 repeatedly. The interference of repelled and refracted droplet light was monitored. Images video fixation procedure was performed by using cross-correlation digital camera 5. Droplet dimension in the gases flow [27] was determined by numbers of interference fringes observed on videograms. Under the IPI method [27] the average values of maximum diameters and typical radius values R_d were calculated, since on videograms the water droplets were presented in ellipsoid shape.

On the second stage of each experiment the power fluid droplet dimension was fixed after its motion through high-temperature gases medium (combustion products flow in the cylindrical conduit 13 at about 1 m in height and 0.3 m in bore). Domain, marked by the "light pulse" of laser in cross-correlation digital camera focus, was selected under the cylinder 13, respectively. Droplet dimension at the end of cylinder was fixed the same way as it was at the first stage of experiment. The comparison of the power fluid droplet dimension was conducted before (R_d) and after (R_d^*) its motion through high-temperature gases medium.

Also the values of entrance (V_d) and output (V_d^*) droplet velocity in the high-temperature gases medium were determined during the experiment videograms processing. Droplet velocity measurement is based on measurement of admixture particle motion in the fixed time interval ($0.1 \cdot 10^{-3}$ s between laser bursts) [26–28], "tracers." They were founded in section plane of laser experimental domain and cross-correlation digital camera. The PIV method of digitally "tracer" visualization [26, 27] has been used. The averaging procedure of motion velocity of water "tracer" particles was performed for calculation of the water droplet motion velocity.

The random inaccuracies of droplet dimension measurement were not more than 2%. The mean-squared departure of measured dimensions in set of experiments was less than $0.09 \cdot 10^{-3}$ m. The systematic inaccuracy of droplet dimension and velocity measurement was about 0.5% and 1%, respectively.

The values of conditional droplet radius (ellipsoid shape), R_d, were established by using the IPI method during the videograms analysis (typical videograms are in Figure 6). The relative reduction by droplet in passing a given distance through the high-temperature gases medium has been analyzed to comparison of experimental and theoretic droplet dimension values. The variable ΔR which shows the R_d decreasing relative to the initial value has been considered.

Under experiments it has been determined (Table 2) that, after the water droplet moved (the initial velocity is about 1 m/s) 1 m in length through the high-temperature (1080 ± 30 K) gases medium, its dimension reduction was about 25% ($\Delta R \approx 25\%$) if $R_d \approx 0.5 \cdot 10^{-3}$ m. In numerical modeling of single droplets when $R_d = 0.25 \cdot 10^{-3}$ m, $Z_d = 10^{-3}$ m, $V_0 = 1$ m/s it has been established that dimension reduction (the parameter averaging ΔR for two coordinates is executed) was about 22%.

Table 2: Experimental values of dimensions and velocities of single water droplets at it motion thought high-temperature gases.

$R_d \cdot 10^3$, m	0.52	1.03	1.54	2.13	2.52	3.01	3.56
$R_d^* \cdot 10^3$, m	0.39	0.89	1.38	1.87	2.36	2.85	3.41
V_d^*, m/s	0.82	1.15	1.34	1.52	1.74	1.93	2.16

* on an exit from high-temperature gases channel.

Also Table 2 shows the values of the water droplet motion velocity after its moving through the high-temperature gases channel (Figure 5). V_d^* established by experiment were little less (about 10–15%) than values V_d received by modeling. For example, in modeling ($R_d = 0.25 \cdot 10^{-3}$ m, $Z_d = 10^{-3}$ m, $V_0 = 1$ m/s, $c_\chi = 0.54$), it has been determined that when water droplet is passing 1 m in length through the combustion products medium, its motion velocity increased by 2–3 times relative to its initial value 0.5 m/s. In the experiments (Table 2), this velocity increased by 1.5–2.5 times. The analysis of water droplet motion model (4) adopting the conclusion base [13–19] enables us to infer that its development towards opposite of the opposite (or unidirectional) gases motion is expedient. It is exceptionally important in research processes of water droplet motion through gases flows with nonuniform velocity in absolute and vector values.

The configurations of moving droplet surface, ellipsoids (Figure 6), established by experiment, match the experiments results of free-moving droplets [9, 10]. Herewith circular droplet motion has been recorded similarly [9, 10]. Effects of droplet destruction (decay) were not observed in the experiments. This can be explained by the moderate motion velocity (less than 5 m/s). By the analyses of the typical experiment videograms (Figure 6) we can infer that the assumptions to heat and mass transfer model (Figure 1), relating to deformation and droplet decay, are rightful.

Under the gases temperature T_f control in channel 13 of experimental plant (Figure 5) it has been determined that T_f in single droplet motion trace reduced greatly (about several hundred degrees) relative to 1100 K (in evaporation). However, a few (less than 5) seconds after droplet had moved, T_f reached its maximum. This result illustrates relatively small dimension of the "temperature" and "concentration" traces, where the temperature and gases concentration were significantly decreased relative to the initial values. Isolines T (Figure 3) and γ_w (Figure 4), established by numerical modeling, show significant temperature reduction and gases concentration in the close vicinity of the trajectory of droplet motion only.

Considering the difficult influence of the modeling factors, we can infer the satisfactory fit of theoretic and experimental research results and the adequacy of the formulated heat and mass transfer model.

4. Conclusion

It has been considered that in the droplet intensive evaporation its surface configuration influences integral characteristics of heat and mass transfer and the evaporation in the high-temperature gases medium insignificantly. Obtained

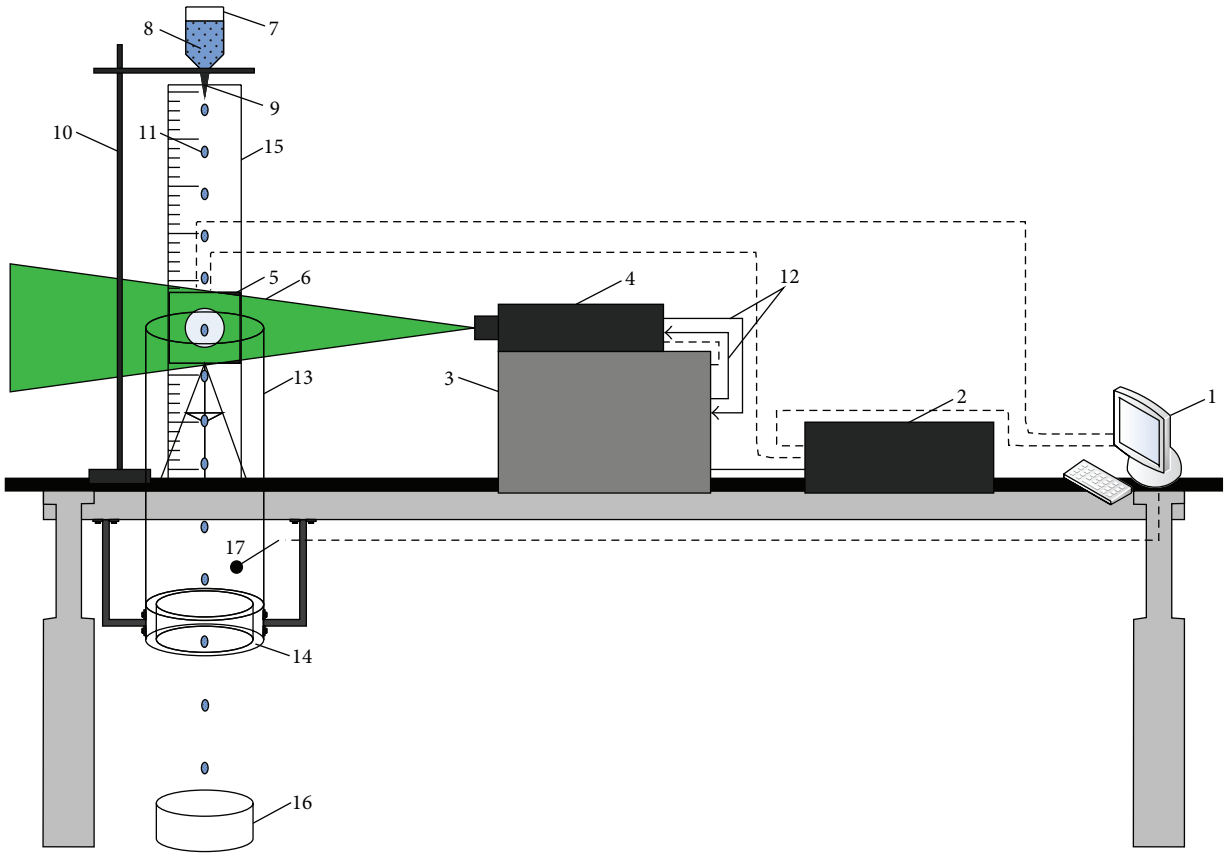

Figure 5: A scheme of experimental plant. 1: personal computer; 2: synchronizer of personal computer, cross-correlation digital camera, and laser; 3: laser generator; 4: solid state lasers for ultrashort pulses; 5: cross-correlation digital camera; 6: light pulse; 7: vessel with experimental liquid; 8: experimental liquid; 9: dosing device; 10: mount; 11: droplets; 12: cooling liquid contour; 13: cylinder from a heat-resistant translucent material; 14: hollow cylinder with combustible liquid in internal medium; 15: measuring grid for determination of a droplet dimension; 16: vessel for collecting liquid; 17: thermocouple.

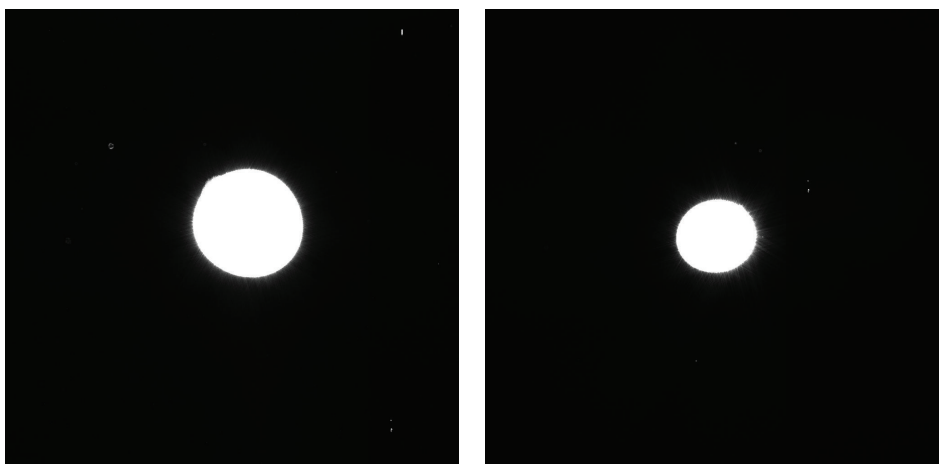

(a) (b)

Figure 6: Videograms of single droplets on an entrance (a) and an exit (b) from high-temperature gases channel at $R_d = 3 \cdot 10^{-3}$ m.

results confirm that it is rightful to use geometric characteristics simplified models with droplets of symmetric bodies revolution shapes, especially cylinders, which is characterized by average values of resistance coefficient c_χ relative to the realistically possible values. It can be realized in the numerical analysis of the water droplet motion regularity through high-temperature gases medium.

Conflict of Interests

The authors declare that there is no conflict of interests regarding the publication of this paper.

Acknowledgment

The reported study was financially supported by grant funds as part of the program to improve the competitiveness of the National Research Tomsk Polytechnic University.

References

[1] R. Wighus, "Water mist fire suppression technology—status and gaps in knowledge," in *Proceedings of the International Water Mist Conference*, pp. 1–26, Vienna, Austria, October 2001.

[2] A. I. Karpov, V. Novozhilov, V. K. Bulgakov, and A. A. Galat, "Numerical modeling of the effect of fine water mist on the small scale flame spreading over solid combustibles," in *Proceedings of the 8th International Symposium on Fire Safety Science*, pp. 753–764, Beijin, China, September 2005.

[3] A. Abbud-Madrid, D. Watson, and J. T. McKinnon, "On the effectiveness of carbon dioxide, nitrogen and water mist for the suppression and extinction of spacecraft fires," in *Proceeding of Suppression and Detection Research and Applications Conference*, Orlando, Fla, USA, March 2007.

[4] T. Carriere, J. R. Butz, S. Naha, A. Brewer, and A. Abbud-Madrid, "Fire suppression test using a handheld water mist extinguisher designed for the international space station," in *Proceeding of 42nd International Conference on Environmental Systems*, Calif, USA, July 2012.

[5] B. Rodriquez and G. Young, "Development of the international space station fine water mist portable fire extinquisher," in *Proceeding of 43rd International Conference on Environmental Systems*, pp. 1–8, Colo, USA, July, 2013.

[6] O. V. Vysokomornaya, G. V. Kuznetsov, and P. A. Strizhak, "Heat and mass transfer in the process of movement of water drops in a high-temperature gas medium," *Journal of Engineering Physics and Thermophysics*, vol. 86, no. 1, pp. 62–68, 2013.

[7] P. A. Strizhak, "Numerical analysis of evaporation process for drop moving at the water jet through high temperature combustion products," *Fire and Explosion Safety*, vol. 21, no. 9, pp. 17–22, 2012 (Russian).

[8] P. A. Strizhak, "Influence of drop distribution in a "water slug" on the temperature and concentration of combustion products in its wake," *Journal of Engineering Physics and Thermophysics*, vol. 86, no. 4, pp. 895–904, 2013.

[9] E. H. Thinh, R. G. Holt, and D. B. Thiessen, "The dynamics of ultrasonically levitated drops in an electric field," *Physics of Fluids*, vol. 8, no. 1, pp. 43–61, 1996.

[10] V. V. Dubrovskii, A. M. Podvysotskii, and A. A. Shraiber, "Measuring natural oscillation periods for droplets and two-component particles," *Journal of Engineering Physics*, vol. 58, no. 5, pp. 622–625, 1990.

[11] G. V. Kuznetsov and P. A. Strizhak, "Effect of the shape of a particle heated to a high temperature on the gas-phase ignition of a liquid film," *Russian Journal of Physical Chemistry B*, vol. 4, no. 2, pp. 249–255, 2010.

[12] D. O. Glushkov and P. A. Strizhak, "Transient heat and mass transfer of liquid droplet ignition at the spreading over the heated substrate," *Advances in Mechanical Engineering*, vol. 2014, Article ID 269321, 9 pages, 2014.

[13] A. B. Basset, "On the motion of a sphere in a vicous liquid," *Philosophical Transactions of the Royal Society of London A: Mathematical and Physical Sciences*, vol. 179, pp. 43–69, 1888.

[14] C. W. Oseen, *Hydromechanik*, Akademische Verlagsgem, Leipzig, Germany, 1927.

[15] A. Haider and O. Levenspiel, "Drag coefficient and terminal velocity of spherical and nonspherical particles," *Powder Technology*, vol. 58, no. 1, pp. 63–70, 1989.

[16] T. L. Thompson and N. N. Clark, "A holistic approach to particle drag prediction," *Powder Technology*, vol. 67, no. 1, pp. 57–66, 1991.

[17] S. Sou, *Hydrodynamics of Multiphase Systems*, Mir, Moscow, Russia, 1971, (Russian).

[18] P. Eisenklam, S. A. Arunachalam, and J. A. Weston, "Evaporation rates and drag resistence of burning drops," in *Proceedings of 11th International Symposium on Combustion*, pp. 715–728, Pittsburg, Pa, USA, 1967.

[19] M. R. Maxey and J. J. Riley, "Equation of motion for a small rigid sphere in a nonuniform flow," *Physics of Fluids*, vol. 26, no. 4, pp. 883–889, 1983.

[20] T. M. Muratova and D. A. Labuntsov, "Kinetic analysis of the evaporation and condensation processes," *Thermal Physics of High Temperatures*, vol. 7, pp. 959–967, 1969.

[21] A. A. Samarskii, *The Theory of Difference Schemes*, Marcel Dekker, 2001.

[22] S. S. Sazhin, W. A. Abdelghaffar, E. M. Sazhina, and M. R. Heikal, "Models for droplet transient heating: effects on droplet evaporation, ignition, and break-up," *International Journal of Thermal Sciences*, vol. 44, no. 7, pp. 610–622, 2005.

[23] S. S. Sazhin, "Advanced models of fuel droplet heating and evaporation," *Progress in Energy and Combustion Science*, vol. 32, no. 2, pp. 162–214, 2006.

[24] N. S. Khabeev, "Duhamel integral form for the interface heat flux between bubble and liquid," *International Journal of Heat and Mass Transfer*, vol. 50, no. 25-26, pp. 5340–5343, 2007.

[25] G. V. Kuznetsov and P. A. Strizhak, "Transient heat and mass transfer at the ignition of vapor and gas mixture by a moving hot particle," *International Journal of Heat and Mass Transfer*, vol. 53, no. 5-6, pp. 923–930, 2010.

[26] J. Westerweel, "Fundamentals of digital particle image velocimetry," *Measurement Science and Technology*, vol. 8, no. 12, pp. 1379–1392, 1997.

[27] M. Raffel, C. Willert, and J. Kompenhans, *Particle Image Velocimetry*, Springer, Berlin, Germany, 1998.

[28] J. M. Foucaut and M. Stanislas, "Some considerations on the accuracy and frequency response of some derivative filters applied to particle image velocimetry vector fields," *Measurement Science and Technology*, vol. 13, no. 7, pp. 1058–1071, 2002.